

## Design of Surface Termination for High-Performance Perovskite Solar Cells

Yan Yang, Wangen Zhao,\* Tengteng Yang, Jiali Liu, Jingru Zhang, Yuankun Fang,  
Shengzhong (Frank) Liu\*

Y. Yang, Prof. W. Zhao, T. Yang, J. Liu, J. Zhang, Y. Fang, Prof. S. Liu

Key Laboratory for Applied Surface and Colloid Chemistry, National Ministry of  
Education; Shaanxi Engineering Lab for Advanced Energy Technology; School of  
Materials Science and Engineering, Shaanxi Normal University, Xi'an 710062,  
China.

Email: [wgzhao@snnu.edu.cn](mailto:wgzhao@snnu.edu.cn); [szliu@dicp.ac.cn](mailto:szliu@dicp.ac.cn)

Prof. S. Liu

Dalian National Laboratory for Clean Energy, iChEM (Collaborative Innovation  
Center of Chemistry for Energy Materials); Dalian Institute of Chemical Physics,  
Chinese Academy of Sciences, Dalian, 116023, China.

Email: [szliu@dicp.ac.cn](mailto:szliu@dicp.ac.cn)

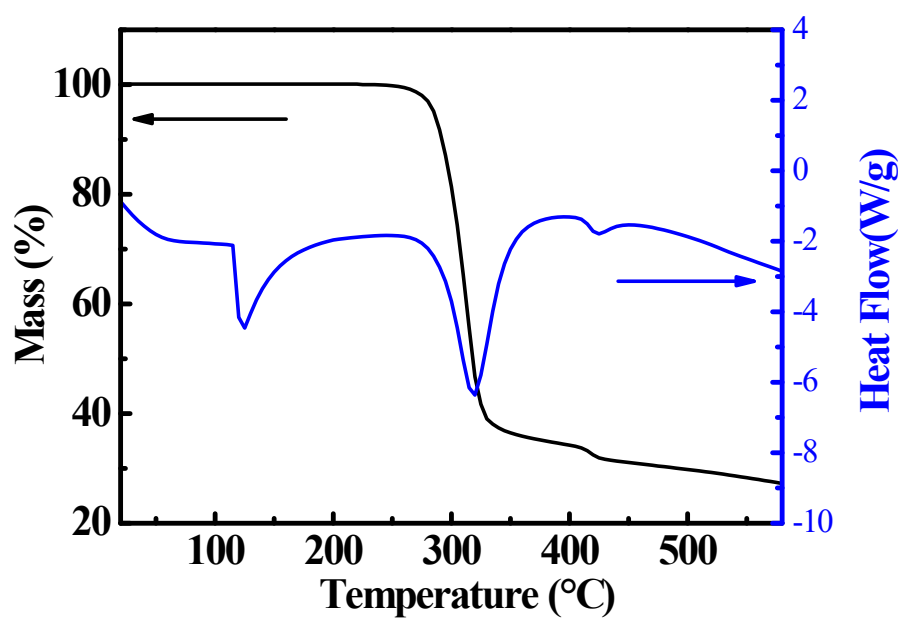


**Fig. 1.** Thermogravimetric analysis (TGA) of GASCN.

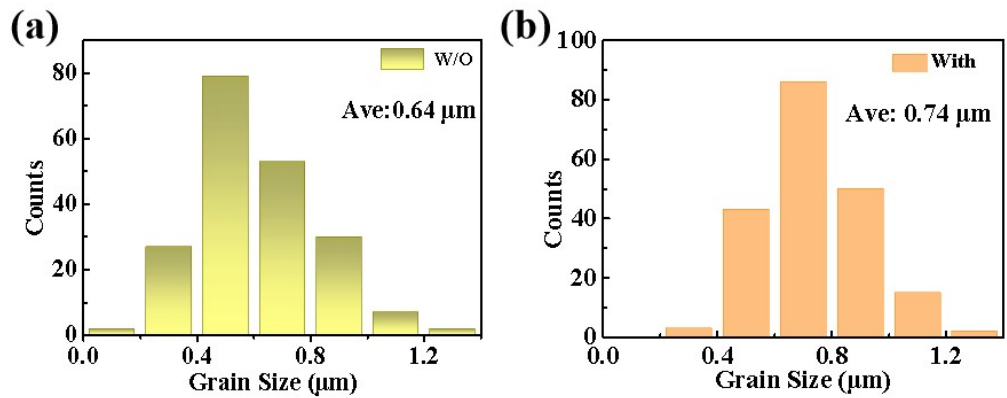


**Fig. 2.** Corresponding statistical size distributions for the  $\text{MAPbI}_3$  films with GASCN contents, respectively. All films were deposited on glass/FTO/c-TiO<sub>2</sub> substrates.

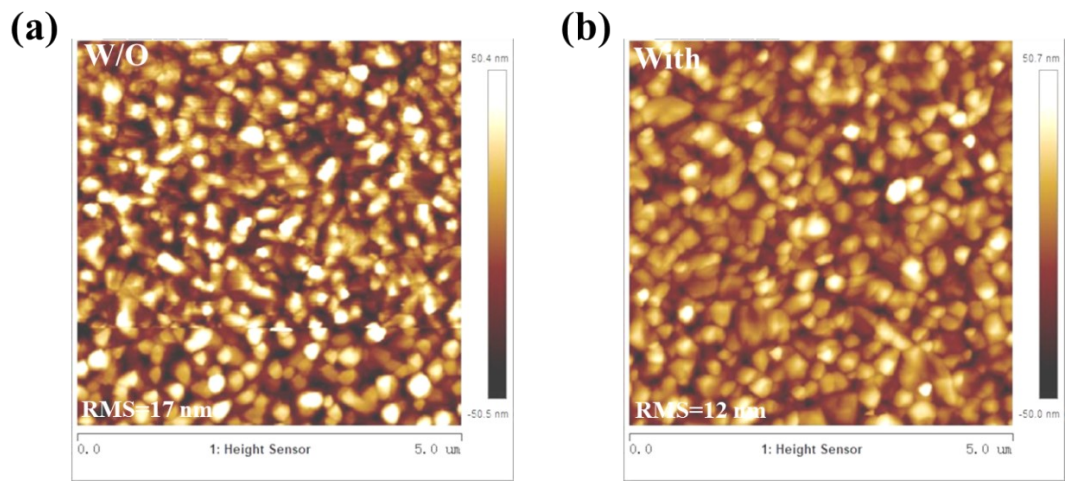


**Fig. 3.** Atomic force microscopy (AFM) images of the pristine and 0.05mg/ml GASCN treated film. The region of the AFM images is  $5 \times 5 \mu\text{m}$ .

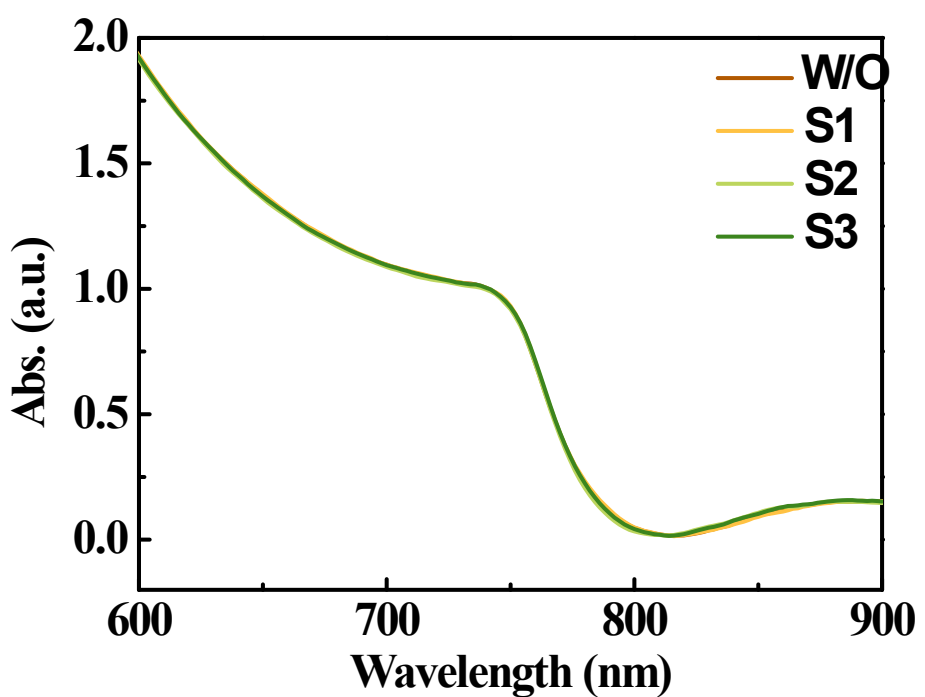


**Fig. 4.** UV-vis absorbance spectrum of the perovskite films with the different amounts of GASCN modification.

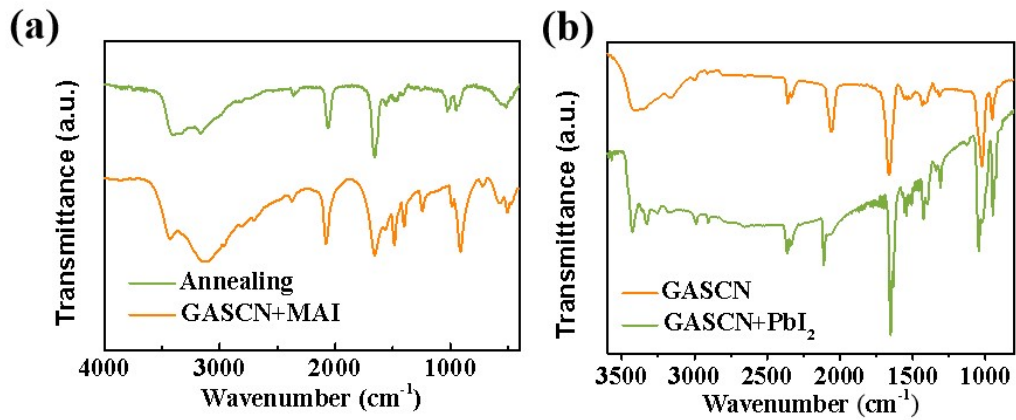


**Fig. 5.** Fourier transform infrared (FTIR) spectra of (a) GASCN and MAI before and after annealing and (b) GASCN with and without PbI<sub>2</sub> in DMSO solutions.

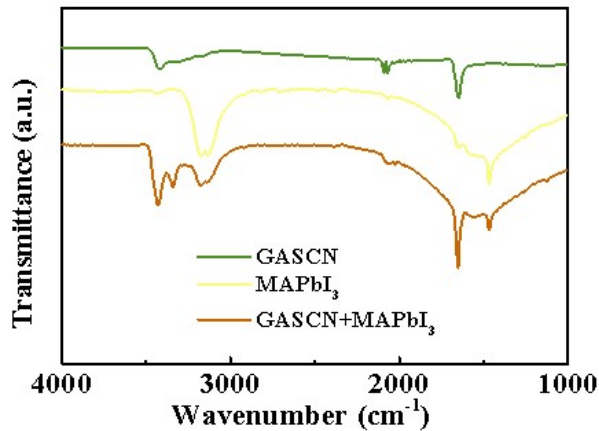


**Fig. 6.** Fourier transform infrared (FTIR) spectra of different films. All films were deposited on glass/FTO/c-TiO<sub>2</sub> substrates.

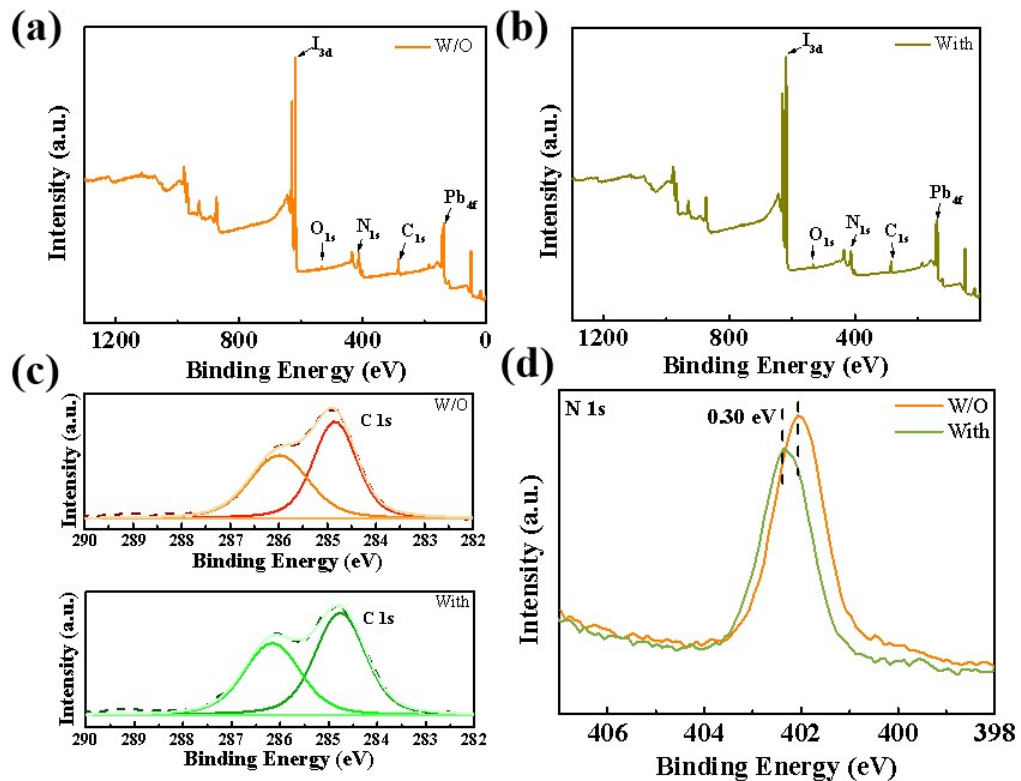


**Fig. 6.** XPS spectra of (a) pristine film and (b) GASCN treated film, and high resolution XPS of C 1s (c) and (d) N 1s of pristine and GASCN-MAPbI<sub>3</sub> films.

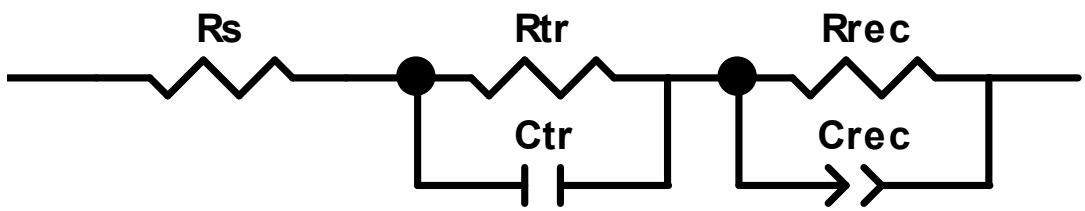


**Fig. 7.** Equivalent circuit model for the EIS spectra at bias voltage of 1.0 V.  $R_s$ ,  $R_{tr}$ ,  $R_{rec}$  and  $C_{rec}$  are series resistance, transport resistance, recombination resistance and the chemical capacitance, respectively.

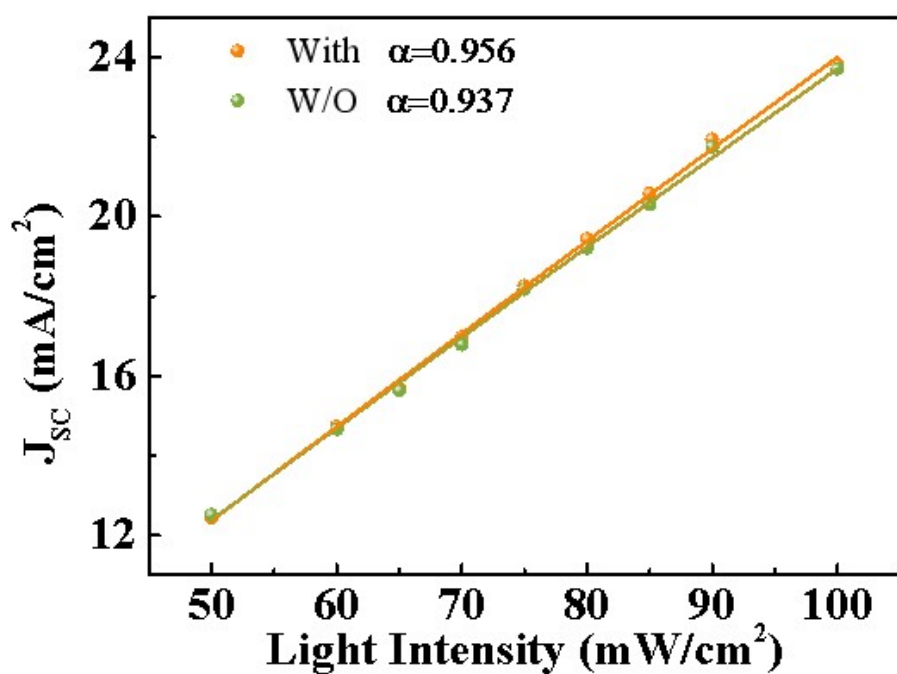


**Fig. 8.** The  $J_{sc}$  as a function of the light intensity for the corresponding devices.

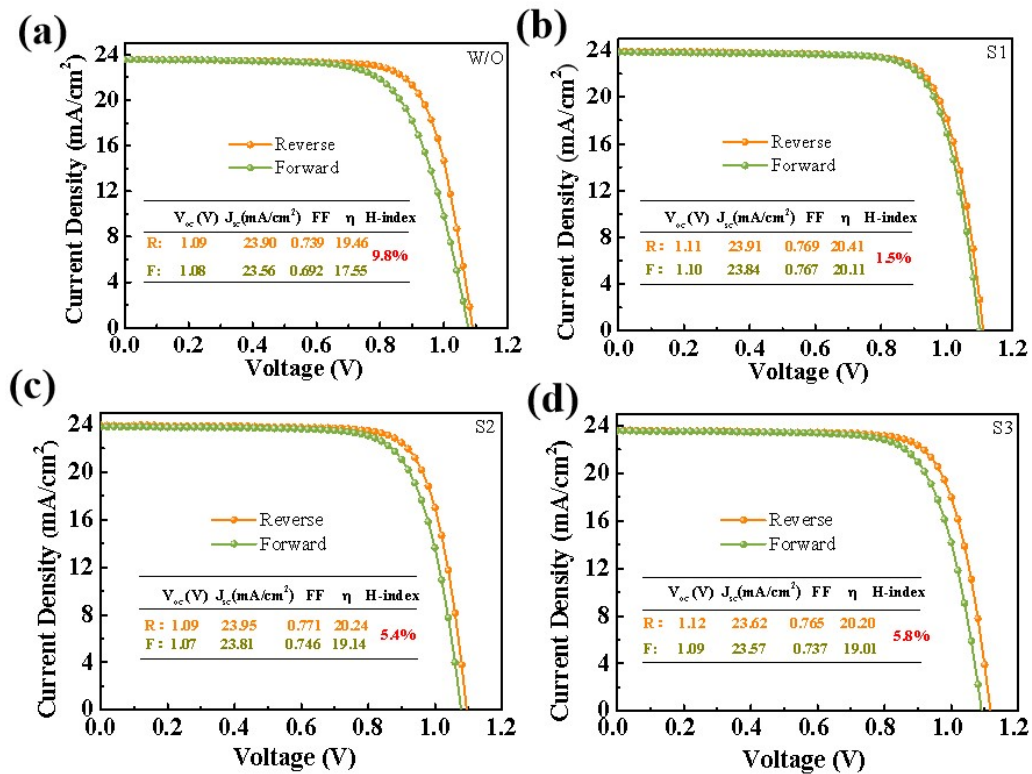


**Fig. 9.** The  $J$ - $V$  curves of  $\text{MAPbI}_3$  perovskite cells without and with GASCN treatment are recorded with forward and reverse voltage scanning directions under AM 1.5G irradiation ( $100 \text{ mW cm}^{-2}$ ).

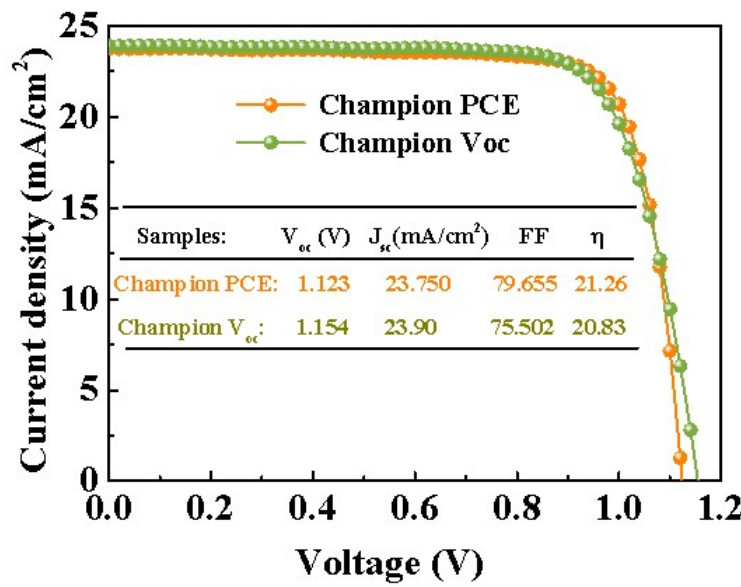


**Fig. 11.**  $J$ - $V$  curve of device with the champion  $V_{OC}$  and champion PCE measured by reverse scan under standard AM 1.5G irradiation.

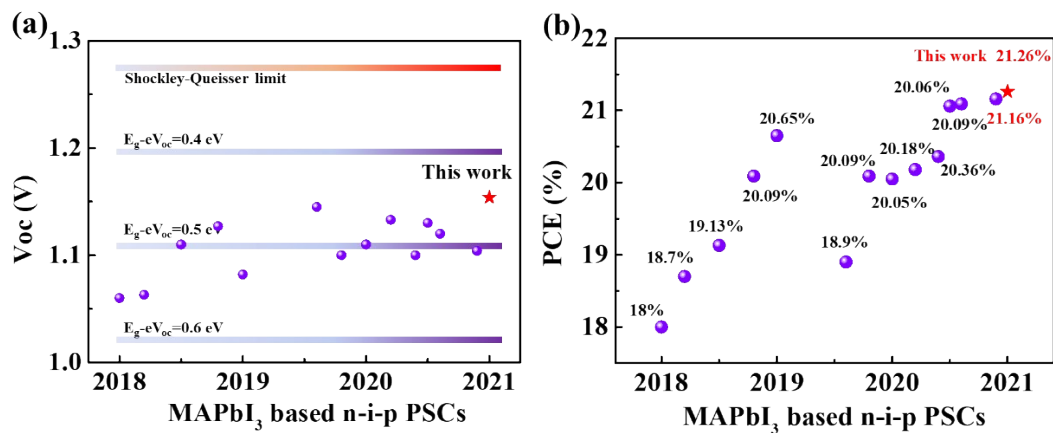


**Fig. S12** Photovoltaic parameters statistics of  $\text{MAPbI}_3$  based n-i-p PCSSs in recent three years.

**Table 1.** Photovoltaic parameters for typical MAPbI<sub>3</sub> devices based on different solvent of GASCN with reverse scanning directions. All *J-V* curves were measured under simulated AM 1.5G illumination with a reverse scan rate of 0.15 V s<sup>-1</sup>.

<b>Sample</b>	<b><i>V<sub>oc</sub></i> (V)</b>	<b><i>J<sub>sc</sub></i> (mA/cm<sup>2</sup>)</b>	<b>Fill Factor (%)</b>	<b>PCE (%)</b>
CH	1.112 (1.103±0.007)	23.99 (23.69±0.18 )	76.54 (74.92±1.46)	20.23 (19.58±0.48)
	1.154 (1.133±0.014)	23.95 (23.81±0.11)	79.65 (77.76±1.14)	21.26 (20.98±0.14)
CB	1.129 (1.100±0.018)	23.98 (23.76±0.17)	75.95 (74.01±1.29)	20.23 (19.35±0.58)
	1.113 (1.083±0.012)	23.99 (23.67±0.16)	74.71 (72.63±1.40)	19.38 (18.61±0.41)
EA				
IPA				

**Table 2.** Fitted parameters based on TR-PL spectra of the perovskite films.

<b>Sample</b>	<b><math>\tau_1</math> (ns)</b>	<b>% of <math>\tau_1</math></b>	<b><math>\tau_2</math> (ns)</b>	<b>% of <math>\tau_2</math></b>	<b><math>\tau_{ave}</math> (ns)</b>
W/O	22.095	37.20	12.808	62.80	22.095
S1	71.545	51.02	33.668	48.98	52.992
S2	65.687	57.86	27.374	42.14	49.540
S3	55.261	51.20	20.975	48.80	38.529

**Table 3.** Equivalent circuit fitting parameters for the EIS spectra.

<b>Sample</b>	<b>R<sub>s</sub> (<math>\Omega</math>)</b>	<b>R<sub>tr</sub> (<math>\Omega</math>)</b>	<b>C<sub>tr</sub> (nF)</b>	<b>R<sub>rec</sub> (<math>\Omega</math>)</b>	<b>C<sub>rec</sub> (nF)</b>
W/O	33.85	124	38.46	3130	12.18
With	33.36	385	71.08	7885	23.45

**Table 4.** Literature survey of recent works on polycrystalline  $\text{MAPbI}_3$ -based n-i-p PSCs.

Device Structure	$J_{sc}$ (mA/cm <sup>2</sup> )	$V_{oc}$ (V)	FF (%)	PCE(%)	Ref.
$\text{SnO}_2/\text{MAPbI}_3/\text{FAI}/\text{HTL}$	22.99	1.127	77.50	20.09	1
c-TiO <sub>2</sub> /m-TiO <sub>2</sub> /MAPbI <sub>3</sub> /AVA/HTL	22.30	1.060	76.00	18.00	2
$\text{SnO}_2/\text{MAPbI}_3/\text{EDBEPbI}_4/\text{HTL}$	23.17	1.110	73.90	19.13	3
$\text{SnO}_2/\text{MAPbI}_3/\text{QA}/\text{HTL}$	23.19	1.130	80.00	21.06	4
c-SnO <sub>2</sub> /MAPbI <sub>3</sub> /HTL	23.98	1.120	78.62	21.09	5
c-SnO <sub>2</sub> /MAPbI <sub>3</sub> /HTL	23.73	1.100	78.00	20.36	6
Li-SnO <sub>2</sub> /MAPbI <sub>3</sub> /HTL	23.24	1.133	76.66	20.18	7
c-TiO <sub>2</sub> /SnO <sub>2</sub> /MAPbI <sub>3</sub> /HTL	23.39	1.104	81.90	21.16	8
c-TiO <sub>2</sub> /SnO <sub>2</sub> /MAPbI <sub>3</sub> /HTL	22.92	1.110	79.00	20.05	9
c-TiO <sub>2</sub> /MAPbI <sub>3-x</sub> Cl <sub>x</sub> /HTL	21.91	1.063	80.00	18.70	10
$\text{SnO}_2/\text{Chol-SnO}_2/\text{MAPbI}_3/\text{HTL}$	22.80	1.145	72.41	18.90	11
c-TiO <sub>2</sub> /MAPbI <sub>3</sub> /HTL	23.89	1.100	76.40	20.09	12
c-TiO <sub>2</sub> /SnO <sub>2</sub> /MAPbI <sub>3</sub> /HTL	23.31	1.082	82.25	20.65	13
TiO <sub>2</sub> /MAPbI <sub>3</sub> /HTL	23.75	1.123 1.154 (highest)	79.66	21.26	This work

Respectively, all HTL in the table refer to Spiro-OMeTAD.

**References:**

- 1 Y. Zou, H.-Y. Wang, Y. Qin, C. Mu, Q. Li, D. Xu and J. Zhang, *Adv. Funct. Mater.*, 2019, **29**, 1805810.
- 2 T. Ye, A. Bruno, G. Han, T. M. Koh, J. Li, N. F. Jamaludin, C. Soci, S. G. Mhaisalkar and W. L. Leong, *Adv. Funct. Mater.*, 2018, **28**, 1801654.
- 3 P. Li, Y. Zhang, C. Liang, G. Xing, X. Liu, F. Li, X. Liu, X. Hu, G. Shao and Y. Song, *Adv. Mater.*, 2018, **30**, e1805323.
- 4 Q. He, M. Worku, H. Liu, E. Lochner, A. J. Robb, S. Lteif, J. S. R. Vellore-Winfred, K. Hanson, J. B. Schlenoff, B. J. Kim and B. Ma, *Angew. Chem. Int. Ed.*, 2021, **60**, 2485-2492.
- 5 Z. Liu, F. Cao, M. Wang, M. Wang and L. Li, *Angew. Chem. Int. Ed.*, 2020, **59**, 4161-4167.
- 6 W. Hou, G. Han, T. Ou, Y. Xiao and Q. Chen, *Angew. Chem. Int. Ed.*, 2020, **59**, 21409-21413.
- 7 K. Jung, W.-S. Chae, J. W. Choi, K. C. Kim and M.-J. Lee, *J. Energy Chem.*, 2020, **59**, 755-762.
- 8 X. Wang, Y. Wang, T. Zhang, X. Liu and Y. Zhao, *Angew. Chem. Int. Ed.*, 2020, **59**, 1469-1473.
- 9 N. Wei, Y. Chen, Y. Miao, T. Zhang, X. Wang, H. Wei and Y. Zhao, *J. Phys. Chem. Lett.*, 2020, **11**, 8170-8176.
- 10 F. Wu, X. Yue, Q. Song and L. Zhu, *Sol. RRL.*, 2018, **2**, 1700147.
- 11 J. Yan, Z. Lin, Q. Cai, X. Wen and C. Mu, *ACS Appl. Energy Mater.*, 2020, **3**, 3504-3511.

- 12 Z. Yao, W. Zhao, Z. Xu, J. Wen and S. Liu, *Small*, 2020, **16**, e2003582.
- 13 Y. Wang, H. Zhang, T. Zhang, W. Shi, M. Kan, J. Chen and Y. Zhao, *Sol. RRL.*,  
2019, **3**, 1900197.